JOURNAL OF AIRCRAFT
Vol. 39, No. 5, September–October 2002

Quantitative Measurements of Wake Vortex Motion in a Water Tunnel

Kamran Rokhsaz* and Renaud Rebours†
Wichita State University, Wichita, Kansas 67260-0044
and
Scott R. Foster‡
Cessna Aircraft Company, Wichita, Kansas 67277

A novel technique is presented for quantitative data acquisition regarding the motion of a pair of vortex filaments in a water tunnel. This technique allows measuring the vortex strength, the oscillation frequency of the vortex filaments, and the rate of growth of their amplitudes simultaneously. The filaments are visualized using dye injection while their cross sections are illuminated with light sheets at different downstream locations and recorded. Time history of the vortex position is extracted from these recordings. This measurement technique is shown to be a viable method of analyzing wake vortex motion. Pairs of vortex filaments, typical of those of wingtips, are used in a water tunnel to demonstrate the application of the method. Vortex strength and the distance between the filaments are varied independently, and the motions of the vortex pairs are quantified. The method is shown to be robust and reliable, as long as the dye remains in the vortex core.

Nomenclature

a	=	amplitude growth rate
b_v	=	separation between vortices, vortex span
C	=	chord length
I	=	moment of inertia
I_c	=	moment of inertia about centroid
$I_{\min/\max}$	=	principal moments of inertia
k	=	wave number
N	=	total number of samples
t	=	time
V_∞	=	freestream velocity
w	=	downwash velocity
x, y, z	=	streamwise, spanwise, and vertical axes
β	=	nondimensional wave number, kb_v
Γ	=	vortex strength
γ	=	nondimensional circulation, Γ/CV_∞
θ_p	=	principal axis inclination angle
τ	=	nondimensional time, tV_∞/C
ω	=	frequency, rad/s

Introduction

IN 1907, Lanchester[1] introduced the concept of tip vortex in an attempt to explain the observed difference in lift between two- and three-dimensional flows. Wingtip vortices have been the subject of a wide range of research ever since, for a variety of purposes. The bulk of the work in this area has been aimed at induced drag reduction by weakening or dispersing of these vortices in the immediate vicinity of the aircraft, or extraction of some of the energy contained within the intensely rotational flowfield. Some of these efforts are outlined in Ref. 2.

Presented as Paper 2001-0111 at the AIAA 39th Aerospace Sciences Meeting, Reno, NV, 15–18 January 2001; received 16 April 2001; revision received 7 June 2001; accepted for publication 10 June 2002.

*Associate Professor, Department of Aerospace Engineering. Associate Fellow AIAA.
†Research Assistant, Department of Aerospace Engineering. Student Member AIAA.
‡Associate Engineer, Engineering Flight Test. Member AIAA.

Research on aircraft wake vortex assumed a state of urgency with the advent of large transport aircraft. Aircraft wake vortex hazard became a safety issue and the dominant criterion for air traffic separation. A comprehensive bibliography of research on aircraft wake vortex hazard is presented in Ref. 3.

Among the efforts cited in Ref. 3 are Refs. 4–8 where the strong influence of the wake vortex of a transport aircraft on a trailing aircraft was studied through a rather large set of flight tests. These tests were conducted to assess the wake location, its persistence, its apparent density, and its effect on the response of trailing aircraft. This research demonstrated the notorious longevity of wake vortices. They showed clearly that the natural aging process, or simple viscous dissipation, takes an unacceptably long time to weaken the vortex to the point of rendering it safe for penetration by other aircraft. Therefore, emphasis was shifted to methods that promised amplification of dynamic instabilities.

Before the 1970s, aircraft wake vortex instability was observed visually and attributed to a variety of factors, including natural turbulence and thermal stratification in the atmosphere. Crow,[9] in his landmark paper, offered an explanation for a form of dynamic instability that could lead to wake vortex breakdown. His analysis showed that, under the right set of conditions, the mutual interaction between two vortex filaments could lead to instabilities whose amplitude would grow with time exponentially. His formulation relied on exponential stability analysis and showed that there are two modes associated with these instabilities: symmetric and antisymmetric. In each case, the growth rate of the amplitude is characterized by the factor e^{at}, where in the unstable cases a is a positive number. His analysis and subsequent research in this area showed that in the symmetric mode, maximum value of the nondimensional form of this parameter is between 0.8 and 1.2. The maximum growth rate depends on the nondimensional wave number β. In the two-filament model, considered by Crow, the vortex span is the same as the distance separating the filaments. The maximum growth rate of the amplitude occurs for β between 0.8 and 2, the higher values corresponding to the antisymmetric mode that has a slightly larger growth rate. Crow showed that the growth rate of the amplitude, and its associated frequency, depended on the choice of an arbitrary cutoff distance. This parameter was required to avoid strong singularities in the governing integrals. Crow discussed the rationale for the choice of this parameter, but arrived at no concrete conclusion regarding its value. Parks[10] showed that these singularities could be avoided if the vorticity is distributed in the core region, without any

necessity for a cutoff distance. Nonetheless, both methods contained inherent uncertainties due to the treatment of these integrals.

Many investigators have studied the application of Crow[9] instability for accelerating the self-destruction of wake vortices with some success. These efforts have included reshaping of the spanwise lift distribution,[11] placing vortex generating fins on the wings,[12] and even harmonically moving control surfaces.[13] All of these techniques proved qualitatively effective in inducing Crow[9] instability and/or reduction of the peak velocities in the wake.

Qualitative examples of Crow[9] instability are abundant in the technical literature, including in the cited references. However, quantitative data, despite the age of the theory, is quite sparse, as is also noted by Leweke and Williamson.[14] This phenomenon has been observed mostly in the atmosphere in conjunction with flight tests, where experimental uncertainties abound. There have been very few tests in the laboratory environment to measure the growth rate of Crow[9] instabilities due to four primary obstacles.

First, Crow[9] instability is a long wave motion that requires long distances to develop significantly enough to be measured accurately. This problem has led some researchers to use tow tanks instead of tunnels. Examples of such work are those of Ciffone and Orloff,[15] Lezius,[16] and Jacob et al.[17] Whereas it is true that in a tow tank the behavior of the vortex filaments can be observed over a very long time, that is, very far away from the point of origin, the amplitude of motion has to be determined visually. Also, in a tow tank, because of physical size limitations, the trailing vortices eventually approach the bottom of the tank, resulting in strong ground effects. In any event, the cited references did not present any results correlating the rate of growth of amplitude with frequency.

Correlation of the amplitude and the frequency is the second source of trouble in quantitative verification of Crow[9] instability. As stated earlier, the rate of growth of amplitude in unstable cases varies with frequency. Eliason et al.[18] used an 80-ft-long wind tunnel with a vibrating plate to excite specific frequencies to examine this correlation. This method allowed the investigators to choose the frequency accurately, but they had to determine the amplitude of motion visually. Consequently, their results fell somewhere in the envelope defined by Crow's[9] theory, yet not conclusively replicating it.

The third source of experimental challenge is the accurate measurement of the vortex strength. The primary reasons are the transient motion of the vortex filament and the viscous effects in any real fluid. A single vortex filament undergoes a self-induced type of motion that is not harmonic, as shown by Rokhsaz et al.[19] This type of motion is present, in addition to that due to mutual induction, in a flowfield containing two vortex filaments. In any case, the vortex motion renders evaluation of the velocity components difficult at best. Furthermore, in the presence of viscous effects, it is not clear how to define the edge of the viscous core and, therefore, extract the vortex strength from the measured velocities.

Finally, in a wind or water tunnel, vortex generation by wings is not practical. At low speeds, where the wake motion can be accurately observed, a single wing cannot generate strong enough vortices for the purpose of accurate flow measurement. On the other hand, higher levels of turbulence that introduce additional elements into the picture invariably accompany higher speeds. To overcome these difficulties Davenport et al.[20] and the present authors used two separate wings for generating the vortices. This method allowed controlling the vortex strength and the distance between the vortices separately. However, the instrumentation used in the two studies was vastly different. Davenport et al.[20] used hot-wire anemometry, whereas in the present study measurements were taken from digital video images.

In the present paper, the authors discuss and demonstrate a simple system that allows quantitative examination of the interactions between a pair of vortex filaments in a water tunnel, using consumer-grade off-the-shelf digital video equipment. The method relies on flow visualization by dye injection in the flow. The locations of the cross sections of the vortex filaments, illuminated with a light sheet, are recorded with a digital video camera. The processing of the video images then results in a wealth of information about the behavior of the filaments in time and in space. The method is described through its application to analyze the motion of several vortex filament pairs.

Experimental Apparatus

Test Facility

The work described here was performed in the water tunnel at the National Institute for Aviation Research (NIAR), located on the campus of Wichita State University (WSU). This facility is a closed-loop horizontal tunnel containing approximately 3500 gal (13.5 m^8) of water. The clear test section, visible from five directions, is 2 ft deep, 3 ft high, and 6 ft (61 × 91 × 18 cm) long. A 2.5-ft (75 cm) segment with constant cross-sectional area connects the test section to the diffuser. This section can also be used as an extension of the test section, allowing observation of a vortex filament over a length of approximately 8 ft (2.44 m). Water speed can be varied from 0.05 to 1.0 ft/s (1.5 to 30.5 cm/s) with very low levels of turbulence. However, the flow speeds of 0.2–0.6 ft/s (6 to 18 cm/s) contain the least amount of turbulence.

The majority of the runs used for the current research were made at tunnel speeds of approximately 0.3 ft/s (9.1 cm/s), corresponding to Reynolds numbers of 3×10^4/ft (9.8×10^4 m). The lowest level of freestream turbulence was visually observed in the neighborhood of this speed, which also corresponded to the lowest tunnel vibration levels measured with an accelerometer. Flow visualization is primarily performed by dye injection, but hydrogen bubbles can also be used for this purpose. Figure 1 shows the schematic of this facility.

Vortex Generation and Visualization

The vortex generating system was composed of two rectangular flat blades, mounted on a reflection plane that was located approximately 4 in. (10 cm) below the free surface of the water. Each blade was made of $\frac{1}{16}$-in.-thick (1.5 mm) aluminum with the chord length of 8.1 in. (20.6 cm) and the span of 12 in. (30.5 cm). The blade incidence angles could be set independently for any arbitrary distance between the two vortex filaments. This arrangement allowed control of the strength of each vortex filament and the virtual span separating the two blades independently. Figure 2 shows the blades and a typical dye stream trailing them. To model the behavior of wing tip vortices, the two blades were set at equal and opposite angles relative to the freestream.

Tip vortices were visualized through dye injection near the leading edge at the blade tips. The objective was to illuminate the cross section of the vortex filaments and to record their motion from the window downstream of the test section. Regular dye made of food coloring proved inappropriate for this purpose because the material was transparent and did not scatter the light. Injecting diluted milk into the vortex cores proved to be the most suitable method

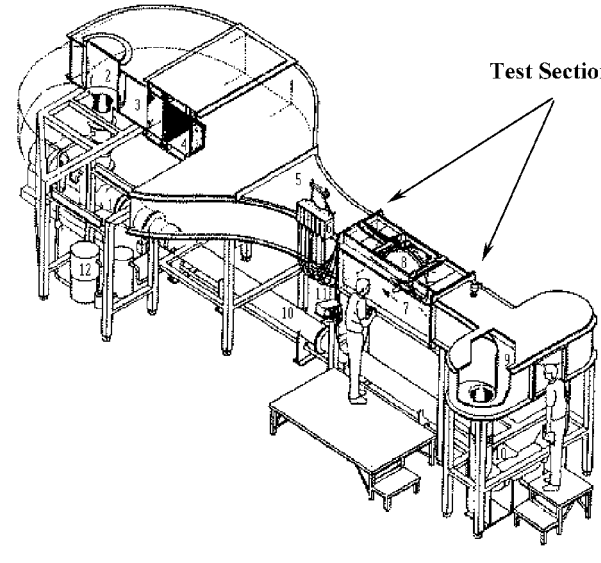

Fig. 1 Schematic view of the WSU/NIAR water tunnel.

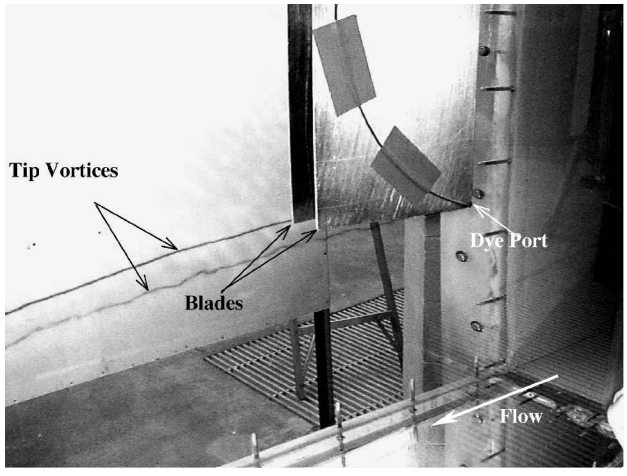

Closeup view

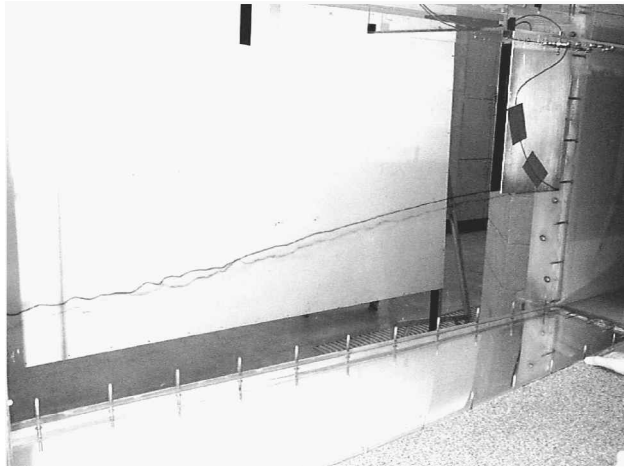

Full view

Fig. 2 Vortex generating blades in the water tunnel.

Fig. 3 Example video frame showing illuminated vortex cores.

of visualizing their motion. When viewed through the downstream window of the tunnel, this technique produced two bright spots, representing the cores, against the dark background that could be recorded on digital videotape. A typical video frame, showing the illuminated vortex cores, is presented in Fig. 3. The light sheet used for this purpose was a $\frac{1}{16}$-in.-thick (1.5 mm) simple high-intensity white parallel beam perpendicular to the test section.

Video Equipment

A Sony™ DCR-TRV120 8-mm digital camcorder was used for recording the vortex motion at 30 frames/s. Each recording was made over 140 s; resulting in 4200 frames. This length represented a compromise between the space available on the hard drive and the number of points needed for fast Fourier transform (FFT) of the data. After the vortex motion was recorded at a specific downstream location, a calibration grid was introduced inside the water tunnel at that location. This grid of 2×2 in. (5×5 cm) squares was then recorded on tape for a few seconds to provide a scale for the vortex motion at this specific downstream location. The resulting video was transformed into the audio–video interleaved (AVI) file format using a PS-Y5028 Miro Video DV-200 card and processed by a Visual Basic code written in house. The processing consisted of locating the bright spots in each frame corresponding to the location of the vortices and recording their coordinates in a file for further analysis. The total duration and the sample rate were such that all frequencies of interest could be extracted without difficulty. All processing was performed on a personal computer with a 450-MHz Pentium processor.

Data Acquisition

A computer code was developed to process the AVI files automatically for extraction of the time history of the vortex motion. The code searched each video frame for the location of the bright spots corresponding to vortex cross sections. The algorithm used here was composed of several steps, each requiring a manual input.

Search Algorithm

In the search stage, the code would step through the video file frame by frame, searching for the white spots representing the vortex cores. These white spots constituted regions of approximately 20 pixels on each side. The search would start with manual input of the core positions in the first frame via the cursor position, providing the code with an initial set of coordinates. To find these points in the subsequent frames, instead of looking through the entire picture, which would be time consuming, the code would look only inside a box of predetermined size. The size of this box was typically between 50×50 and 70×70 pixels, determined by trial and error, according to how much the vortex cores moved from one frame to the next. In the first frame, these boxes were centered on the points picked by the user, whereas in subsequent frames, the code would center this box on the vortex position determined from the previous frame.

The process of locating the vortex cores within the search areas proved to be more complex than it first appeared and needed to be refined several times. Figure 4 shows three examples of how the vortex cores appeared in the video frames. Obviously, the core was not always as well defined as one would have liked it to be. The first type of white spot was ideal (Fig. 4a), it was bright, well contrasted with the background, and almost round. The second type (Fig. 4b) was still bright, but its bean shape made it harder to identify the core. The third type (Fig. 4c) was the hardest one to process because it was very elongated with very low brightness.

Types two and three were the result of a rapid and sometimes whipping motion of the vortex cores. Anything worse than case 3 meant that the dye was dispersing so that the cores could not be visualized and no data could be obtained from that case. Unfortunately, as with all experimental work, the ideal case was a rare occurrence, and so the code was made to account for less-than-perfect case as well.

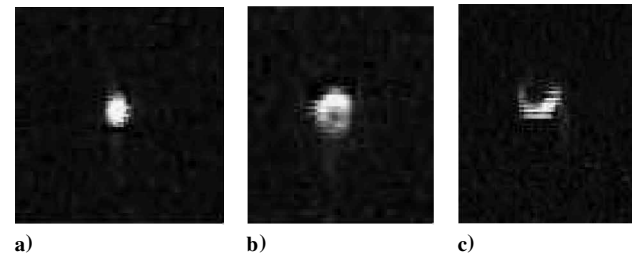

a) b) c)

Fig. 4 Three types of vortex visualization.

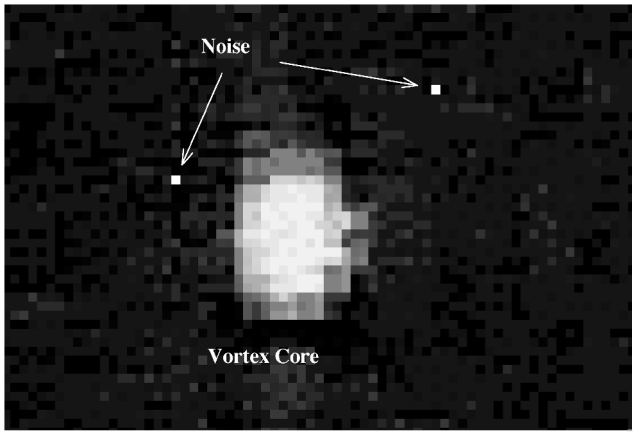

Fig. 5 Background noise before filtering.

Image Filtering

Filtering out the background noise in the search area preceded the search step. Although the background appeared completely dark to the naked eye, Fig. 5 shows that on the pixel scale, some points were almost as bright as the vortex core and could easily be mistaken for it by the computer code. What differentiated noise from the actual vortex core was that a bright pixel that was part of the background noise was usually isolated and surrounded by darker pixels, whereas a bright pixel belonging to the vortex core was neighbored by other bright pixels. Therefore, the filtering operation consisted of replacing the brightness value of every pixel within the search area by the average brightness of a certain area around that pixel. The dimensions of this area were to be provided by the user and, for most cases shown here, were chosen as 9×9 pixels. This operation effectively filtered out the background noise and transformed the existing array of pixels into a new array with new assigned brightness values for each pixel.

A by-product of the filtering was smearing of the vortex images at their edges. Therefore, during the search, the brightness value of each pixel inside the search area was compared to a cutoff value predetermined by the user. If the brightness value of a pixel was greater than the cutoff value, then the pixel was assumed to belong to the vortex image. The geometric centroid of all of the eligible pixels in the search area was assumed to be the vortex core location.

Calibration

The transformation between the pixel coordinates and the physical coordinates was performed using a calibration file. The AVI calibration file consisted of the image of a grid that was placed in the test section at the conclusion of each recording for each downstream location. The code was written to require the user to locate manually two points on the 2×2 in. (5×5 cm) calibration grid. Because it was known that the actual spacing between the points was 2 in. (5 cm) the code would determine the number of pixels corresponding to every inch of actual spacing for that particular downstream location. The number of pixels corresponding to every inch in the physical domain depended on the distance between the grid and the camera, as well as on the zoom setting. However, in most cases, every inch of the physical space corresponded to approximately 100 pixels (40 pixels/cm).

The calibration file was also used to determine an absolute reference for each of the data sets. In other words, the calibration process did not only provide a scale, but the actual positions of the vortex cores in space, measured in a coordinate system fixed to the tunnel. To ensure that this coordinate system remained invariant between different downstream distances, the calibration grid had to be placed at exactly the same location in the water tunnel every time with respect to the floor and one of the sidewalls.

Method of Analysis

After the vortex coordinates were extracted from the video, the data had to be processed to yield meaningful information about the vortex motion. Again, in each video frame, the vortex core location was assumed to be that of the centroid of the collection of pixels whose brightness exceeded a predefined threshold. The locations and the time histories of the centroids for the two vortices, obtained at several downstream locations, provided very important information about the interaction between the two. The reader is reminded that in excess of 4000 frames were used at each downstream location for the following analysis.

Vortex Strength

The separation distance between the two vortices b_v was easily obtained from the distance between their two centroids. This quantity was needed to determine the vortex strength and was also used to nondimensionalize several parameters. For each filament, the difference between the vertical positions of the centroid between every two consecutive downstream locations was used to determine the downwash w acting on the vortex filaments. Because the readings were taken at distances many times the span downstream of the blades, vortex strength was assumed to be related to downwash via

$$w = \Gamma/2\pi b_v = V_\infty(\Delta z/\Delta x) \tag{1}$$

Planes and Amplitude of Motion

The moments of inertia of the pixels in the centroidal axes were used to determine the orientation of the planes in which the oscillatory vortex motions were predominant. By analogy with mass moments of inertia, the following quantities were defined:

$$I_{xx} = \sum_i y_{c_i}^2 \tag{2}$$

$$I_{yy} = \sum_i x_{c_i}^2 \tag{3}$$

$$I_{xy} = \sum_i x_{c_i} y_{c_i} \tag{4}$$

In these summations, each pixel was assigned unit mass, regardless of its brightness level. The principal moments of inertia and the orientation of the associated principal axes were then determined from

$$\theta_p = \frac{1}{2}\tan^{-1}\left[\frac{-I_{xy}}{(I_{xx} - I_{yy})/2}\right] \tag{5}$$

$$I_{\max/\min} = \frac{I_{xx} + I_{yy}}{2} \pm \sqrt{\left(\frac{I_{xx} - I_{yy}}{2}\right)^2 + I_{xy}^2} \tag{6}$$

The axis of the minimum moment of inertia corresponded to the direction along which the vortex moved with the largest amplitude and was a direct indicator of the inclination of the planes of oscillation of Crow[9] waves.

The moments of inertia also provided information about the amplitude of motion of the vortex cores. The root mean square (rms) of the projection of the position of the vortex cores on the axis of minimum moment of inertia was directly related to the maximum moment of inertia and could, therefore, be computed easily according to the following equation:

$$\text{rms} = \sqrt{I_{\max}/N} \tag{7}$$

This rms represented the average amplitude of vortex motion in the inclined planes containing the predominant motion. This information from several downstream distances allowed the analysis of the rate of growth of the amplitude of motion vs the downstream location or the nondimensional frequency β and the correlation of these results with the theory.

Once the projections of the vortex positions on the axis of minimum moment of inertia were obtained, they were used in an FFT analysis. The analysis would identify the dominant frequencies of the vortex motion, if any. This issue will be discussed further in the next section.

Results and Discussion

To demonstrate the fidelity of the described method, a set of tests were performed. The results presented here were obtained for two blade separation distances, two tunnel speeds, and three angles of attack. These combinations are summarized in Table 1. In each case, measurements were made at three different downstream locations in the wake. The closest point to the blades was 15 in. (38.1 cm), that is, $x/C = 1.85$, behind the blades. The farthest point was 40–50 in. (101.6–127 cm) downstream, depending on the angle of attack. The nearest distance was chosen to allow sufficient time for the wake to roll up adequately. Normally, the distance behind the wing, required for complete wake rollup, is several times the wing span. However, in the present cases the rollup process took place rather quickly because of the presence of separated boundary layers over a large part of the blades. The diffusion of the dye prevented clear data acquisition at longer distances.

Figure 6 shows the sink rate of the vortex filaments for cases 1 and 2. Each point in Fig. 6 represents the average of approximately 4000 data points. The nearly constant slope of these curves is a clear indication of the quality of the data and closely matches visual observations made using dye injection. In each case, the vortex strength could be estimated from the combination of the slope and the horizontal separation between the filaments. The latter quantity is shown in Fig. 7. Variations in the slopes of the curves shown in this figure could be attributed to camera movements in between the cases. However, the parameter of importance, the distance between the two filaments, was quite constant. Similar results were obtained for case 3. The resulting vortex strengths and vortex spans are also presented in Table 2. As shown by these results, the measured vortex strength was different for the two filaments. These differences were due to the fact that it was nearly impossible to set the blades at exactly the same angle of attack. However, these differences were very small and did not affect the subsequent results significantly. In the interest of brevity, from this point on, the authors will only discuss the quantitative data pertaining to case 2. See Ref. 21 for further details.

Table 1 Angles of attack and flow speeds

Case	Tunnel speed, ft/s (cm/s)	Blade separation distance, in. (cm)	Blade angle of attack, deg
1	0.30 (9.14)	3.0 (7.62)	6.0
2	0.30 (9.14)	3.0 (7.62)	8.0
4	0.25 (7.62)	4.0 (10.2)	7.0

Table 2 Measured vortex span and vortex strength

Case	Vortex span, in. (cm)	Right vortex γ	Left vortex γ	Percent difference
1	3.02 (7.67)	0.3610	0.3472	4.0
2	2.89 (7.34)	0.4277	0.3931	8.8
3	4.03 (10.24)	0.2287	0.2293	0.2

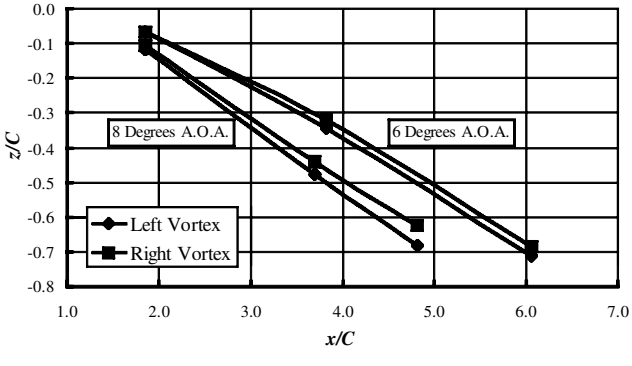

Fig. 6 Depth due to downwash for cases 1 and 2.

Table 3 Amplitude and inclination angles of the planes of motion in degrees for case 2

x/C	θ_p (left), deg	θ_p (right), deg	RMS/C (left)	RMS/C (right)
1.85	−6.29	168.2	0.00559	0.00698
3.70	48.0	145.0	0.02198	0.02490
4.81	65.3	151.2	0.03988	0.05470

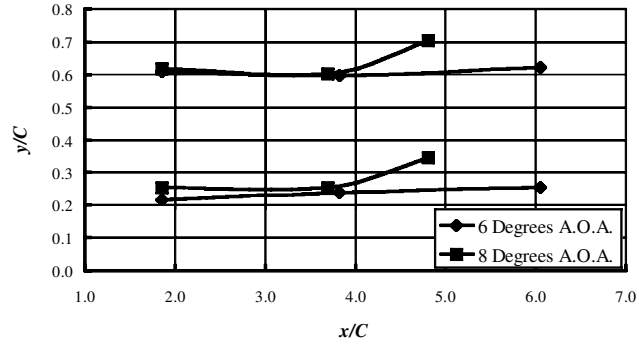

Fig. 7 Horizontal position for cases 1 and 2.

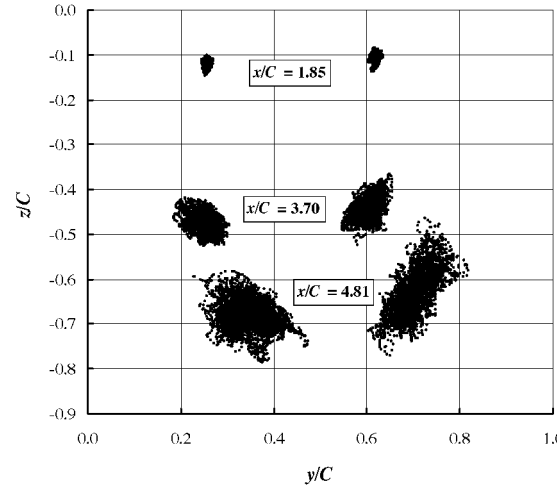

Fig. 8 Rear view of the vortex positions over a 2.5-min period for case 2.

Figure 8 shows the snapshots of the vortex position at three downstream locations for case 2. Figure 8, which contains in excess of 24,000 data points, clearly shows the inclination angles of the planes in which the vortex motion was predominant. These angles were in the same order of magnitude as those predicted by the analytical model of Crow[9] and experimental results of Davenport.[20] These inclination angles, calculated via Eq. (5) are given in Table 3. Judging from the values given in Table 3, the wake did not appear to have completely rolled up at the first downstream distance, that is, $x/C = 1.85$. However, the inclination angles of the other two sets of data were in relatively close agreement. Figure 8 also shows the growth in the amplitude of motion with increasing downstream distance. The rms of the amplitude along the plane of motion for each filament at each downstream distance, evaluated from Eq. (7), is also given in Table 3. These results are entirely consistent with those of Crow.[9]

The stability analysis used by Crow[9] relied on small perturbations and harmonic vortex motion. Figure 9 shows a typical time history of the vortex motion in the vertical direction. The vertical amplitude of motion shown here was approximately 10% of the chord length. This value was in excess of twice the viscous core radius measured earlier[19] and might not qualify as small perturbations. Furthermore, the motion appeared to be harmonic, whereas

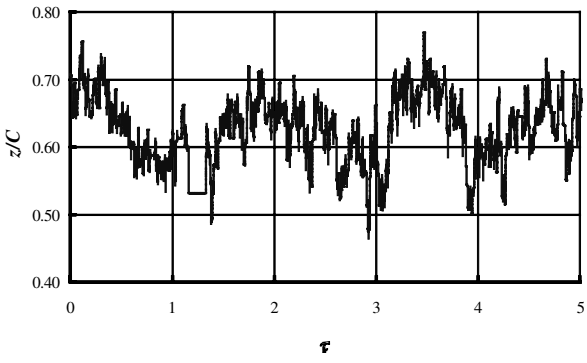

Fig. 9 Time history of the right vortex vertical motion for case 2 at $x/C = 4.81$.

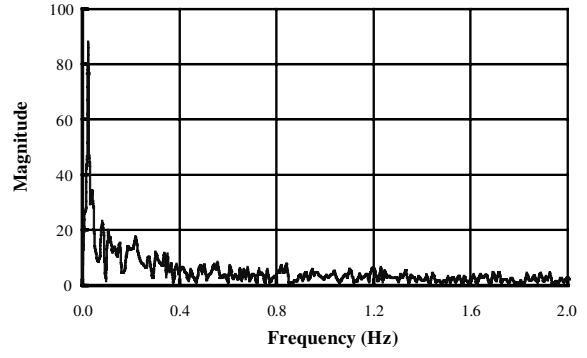

Fig. 10 Coefficients of the Fourier transform of the data from Fig. 9.

Davenport et al.[20] concluded such motion to be random with most of its energy concentrated below the reduced frequency of 1.0. Fourier transform of the data of Fig. 9, shown in Fig. 10, confirms this conclusion. There is a peak corresponding to the frequency of 0.02 Hz in Fig. 10. However, Fourier transforms of same data taken at other downstream distances lacked this peak and resembled random motion more closely. Note that the curve in Fig. 9 remains flat for $1.05 \leq \tau \leq 1.10$ corresponding to a period of 1.3 s in real time. This is the period during which the search algorithm could not track the vortex motion and, thus, locked on to the last known vortex position. This problem would be encountered periodically due to a number of issues such as momentary dye dispersion or severe spiraling of the vortex filament over a short distance. However, such events were of extremely short duration compared with the total recording time (less than 1% of the total period in the present case) and did not compromise the integrity of the data. Nonetheless, the algorithm is being modified to minimize such occurrences.

The results presented here are completely consistent with those of Crow,[9] as well as with other existing experimental data. Therefore, the authors believe that the present approach represents a viable method for analyzing interactions among multiple vortex filaments. Additionally, the strength of the present method lies in its simplicity and its reliance on low-cost equipment.

Conclusions

A novel technique was presented for quantitative measurement of the motion of a pair of vortex filaments in a water tunnel. It was shown that this technique allows measurement of the vortex strength, the oscillatory motion of the vortex filaments, and the rate of growth of their amplitudes simultaneously. Application of this method was demonstrated in a water tunnel, using pairs of vortex filaments, typical of those of wingtips. It was shown clearly that this approach is a viable technique for investigating the interactions among multiple vortex filaments. The method produced reliable and repeatable data, using off-the-shelf hardware for data acquisition. This method is shown to be especially suitable for low-speed studies in water tunnels or water channels where the dominant frequencies are well below 30 Hz. At this writing, no detailed analysis has been performed to examine the degree of error associated with this technique.

Acknowledgments

This work was partially supported by a National Science Foundation grant under the Experimental Program to Stimulate Competitive Research program. The authors would like to express their sincere gratitude to L. Scott Miller for his guidance and for his constructive remarks in performance of this research.

References

[1]Lanchester, F. W., *Aerodynamics—Constituting the First Volume of a Complete Work on Aerial Flight*, A. Constable, London, 1907, pp. 176–178.

[2]Rokhsaz, K., "A Brief Survey of Wing Tip Devices for Drag Reduction," *SAE Transactions*, Vol. 102, Sec. 1, 1994, pp. 1901–1910; also Society of Automotive Engineers, Paper SAE-932574, 1993.

[3]Hallock, J. N., "Aircraft Wake Vortices: An Annotated Bibliography (1923–1990)," Dept. of Transportation–Federal Aviation Administration, Rept. DOT-FAA-RD-90-30, Jan. 1991.

[4]Andrews, W. H., "Flight Evaluation of the Wing Vortex Wake Generated by Large Jet Transports," *Aircraft Wake Turbulence and Its Detection*, edited by J. Olson, A. Goldberg, and M. Rogers, Plenum, New York, 1971, pp. 287, 288.

[5]Andrews, W. H., Drinkwater, F. J., Krier, G. E., and Robinson, G. H., "Flight-Test Evaluation of the Wing Vortex Wake Generated by Large Jet-Transport Aircraft," Compilation of Working Papers on Wake Turbulence Tests, Federal Aviation Administration, Washington, DC, April 1970.

[6]Andrews, W. H., Robinson, G. H., and Larson, R. R., "Aircraft Response to the Wing Trailing Vortices Generated By Large Jet Transports," *Aircraft Safety and Operating Problems*, Vol. 1, NASA-SP-270, 1971, pp. 115–126.

[7]Andrews, W. H., Robinson, G. H., and Larson, R. R., "Flight Investigation of Aircraft Response to the Wing Vortex Wake Generated by Jet Transport Aircraft," NASA TN D-6655, March 1972.

[8]Andrews, W. H., Tymczyszyn, J. J., Jacobson, R. A., and Drinkwater, F. J., "Flight Investigation of the Response of Wide-Body Tri-Jet to the Wing Vortex Wake Generated by Large Transport Aircraft," NASA Flight Research Center, Rept. FWP-35, Edwards, CA, Feb. 1973.

[9]Crow, S. C., "Stability Theory for a Pair of Trailing Vortices," *AIAA Journal*, Vol. 8, No. 12, 1970, pp. 2172–2179.

[10]Parks, P. C., "A New Look at the Dynamics of Vortices with Finite Cores," *Aircraft Wake Turbulence and its Detection*, edited by J. Olson, A. Goldberg, and M. Rogers, Plenum, New York, 1971, pp. 335–388.

[11]Burnham, D. C., "B-747 Vortex Alleviation Flight Tests: Ground-Based Sensor Measurements," Federal Aviation Administration, Rept. FAA-RD-81-99, Jan. 1982.

[12]Rossow, V. J., "Effect of Wing Fins on Lift-Generated Wakes," *Journal of Aircraft*, Vol. 15, No. 3, 1978, pp. 160–167.

[13]Chevalier, H., "Flight Test Studies of the Formation and Dissipation of Trailing Vortices," *Journal of Aircraft*, Vol. 10, No. 1, 1973, pp. 14–18.

[14]Leweke, T., and Williamson, C. H. K., "Long-Wavelength Instability and Reconnection of a Vortex Pair," *Proceedings of the IUTAM Symposium on Dynamics of Slender Vortices*, edited by E. Krause, and K. Gersten, Kluwer Academic, Boston, 1998, pp. 225–234.

[15]Ciffone, D. L., and Orloff, K. L., "Axial Flow Measurements in Trailing Vortices," *AIAA Journal*, Vol. 12, No. 8, 1974, pp. 1154, 1155.

[16]Lezius, D. K., "Water Tank Study of the Decay of Trailing Vortices," *AIAA Journal*, Vol. 12, No. 8, 1974, pp. 1065–1071.

[17]Jacob, J., Savas, O, and Liepmann, D., "Trailing Vortex Wake Growth Characteristics of a High Aspect Ratio Rectangular Airfoil," *AIAA Journal*, Vol. 35, No. 2, 1997, pp. 275–280.

[18]Eliason, B. G., Gartshere, I. S., and Parkinson, G. V., "Wind Tunnel Investigation of Crow Instability," *Journal of Aircraft*, Vol. 12, No. 12, 1975, pp. 985–988.

[19]Rokhsaz, K., Foster, S. R., and Miller, L. S., "Exploratory Study of Aircraft Wake Vortex Filaments in a Water Tunnel," AIAA Paper 99-3199, June 1999.

[20]Davenport, W. J., Zsoldos, J. S., and Vogel, C. M., "The Structure and Development of a Counter-Rotating Wing-Tip Vortex Pair," *Journal of Fluid Mechanics*, Vol. 332, 1997, pp. 71–104.

[21]Rebours, R., *Quantitative Measurements of Crow Instability in a Water Tunnel*, M.S. Thesis, Dept. of Aerospace Engineering, Wichita State Univ., Wichita, KS, Dec. 2000.